Journal of Catalysis 281 (2011) 12–20

Contents lists available at ScienceDirect

Journal of Catalysis

journal homepage: www.elsevier.com/locate/jcat

Switching of reactions between hydrogenation and epoxidation of propene over Au/Ti-based oxides in the presence of H_2 and O_2

Caixia Qi [a,*], Jiahui Huang [b,d], Shuangquan Bao [b], Huijuan Su [a], Tomoki Akita [c,d], Masatake Haruta [b,d,*]

[a] R & D Centre for Gold Industrial Application, Yantai University, Shandong Applied Research Center for Gold Nanotechnology (Au-SDARC), 32 Qingquan Road, Laishan District, Yantai 264005, PR China
[b] Graduate School of Urban Environmental Sciences, Tokyo Metropolitan University, 1-1 Minami-osawa, Hachioji, Tokyo 192-0397, Japan
[c] Research Institute for Ubiquitous Energy Devices, National Institute of Advanced Industrial Science and Technology (AIST), 1-8-31 Midorigaoka, Ikeda, Osaka 563-8577, Japan
[d] Core Research for Exploratory Science and Technology (CREST), Japan Science and Technology Agency (JST), 4-1-8 Hon-cho, Kawaguchi, Saitama 332-0012, Japan

ARTICLE INFO

Article history:
Received 21 December 2010
Revised 27 March 2011
Accepted 29 March 2011
Available online 4 May 2011

Keywords:
Au catalysts
Propene
Epoxidation
Hydrogenation
Reaction switching
Alkaline effect

ABSTRACT

In a H_2 and O_2 mixture, the reaction of propene switches between hydrogenation and epoxidation over Au/Ti-based oxides. Reaction pathways are strongly dependent on the size of Au particles and on the presence of alkalis. The hydrogenation prevails over Au clusters smaller than 2.0 nm (in the absence of alkalis) and over Au nanoparticles larger than 5.0 nm. Alkali contamination can switch hydrogenation to epoxidation over Au clusters and promote epoxidation over Au nanoparticles with diameters of 2.0–5.0 nm. It was also confirmed that the hydrogenation of propene is enhanced by the addition of a small amount of O_2. Switching of product by alkalis and enhancement of hydrogenation by oxygen are interpreted by parallel and competitive reaction pathways.

1. Introduction

Gold surfaces have long been regarded as being chemically inert. However, they exhibit surprisingly high catalytic activity for CO oxidation at a temperature as low as 200 K when Au nanoparticles are deposited on base metal oxides by co-precipitation (CP) or deposition–precipitation (DP) techniques [1,2]. This finding has stimulated catalysis research on Au nanoparticles since the 1990s, and it has been revealed that nanogold catalysts possess excellent activity and selectivity for many chemical reactions [3–6]. A typical example is that Au supported on Ti-containing oxides can catalyze the epoxidation of propene by molecular O_2 in the gas phase with [7–9] or without H_2 [10]. Commercially viable catalytic activity close to 10% yield of propene oxide (PO) over Au/Ti–SiO_2 catalyst systems has recently been achieved by optimizing catalyst formulations [11–14].

In principle, Au nanoparticles and highly dispersed Ti^{4+} in the form of isolated tetrahedral coordination in a SiO_2 matrix are indispensable for PO formation in the presence of H_2 and O_2 [8,9,15]. One surprising feature of the Au/TiO_2 (P-25) catalyst is a switch-like change in product selectivity from PO to propane depending on Au loadings [7]. The product at reaction temperatures below 373 K sharply switched from PO (epoxidation) to propane (hydrogenation) when Au loading was decreased below 0.1 wt.%. The majority of Au particles were smaller than 2.0 nm in diameter. Propane formation at very low gold loadings was also observed over the Au/Ti–MCM-48 catalyst in which the size of Au particles was assumed to be below 2.0 nm [16]. Until now, experimental results have been inconsistent concerning the dependence of the reaction products on the particle size and loading of Au [7,13,14,16–20]; the catalysts with very low Au loadings (<0.05 wt.%) and Au clusters smaller than 2.0 nm prefer PO formation [13,14,17,19,20], while the hydrogenation reaction can take place over larger Au particles with a mean diameter of 8.4 nm and 1 wt.% Au loading [18]. Therefore, it is of great importance to elucidate ruling factors that determine the reaction route to epoxidation or to hydrogenation of propene over Au catalysts.

The co-adsorption of H_2 and O_2 on gold catalysts is an interesting research topic because oxidation reactions can be promoted by H_2, such as preferential CO oxidation [21] and direct epoxidation of propene, while the hydrogenation reaction of propene is enhanced by O_2 over an Au/SiO_2 catalyst [22]. As a matter of fact, there are four competitive reactions that occur simultaneously over Au/Ti-based oxides in the mixture of propene with H_2 and O_2 as shown

* Corresponding authors. Address: Fax: +86 535 6902233 (C. Qi). Graduate School of Urban Environmental Sciences, Tokyo Metropolitan University, 1-1 Minami-osawa, Hachioji, Tokyo 192-0397, Japan. Fax: +81 42 677 2852 (M. Haruta).
E-mail addresses: qicx@ytu.edu.cn (C. Qi), haruta-masatake@center.tmu.ac.jp (M. Haruta).

0021-9517/$ - see front matter © 2011 Elsevier Inc. All rights reserved.
doi:10.1016/j.jcat.2011.03.028

Table 1
Four competitive reactions that occur simultaneously over Au/Ti-based oxides in the mixture of propene with H_2 and O_2.

No.	Type of reaction	Chemical equation	$\Delta_r H^o$ (kJ mol^{-1})	$\Delta_r G^o$ (kJ mol^{-1})	Notes
1	Hydrogen combustion	$H_2 + 1/2O_2 \rightarrow H_2O$	−241.8	−228.6	Major reaction
2	Hydrogenation of propene	$C_3H_6 + H_2 \rightarrow C_3H_8$	−124.3	−86.2	Second major
3	Complete oxidation of propene	$C_3H_6 + 9/2O_2 \rightarrow 3CO_2 + 3H_2O$	−1925.9	−1931.6	At high temperatures
4	Epoxidation of propene	$C_3H_6 + O_2 + H_2 \rightarrow C_3H_6O + H_2O$	−355.0	−317.1	Limited reaction

in Table 1. Since the combustion of propene to CO_2 and water usually needs temperatures much higher than the optimum temperature range for PO or propane formation, the combustion of hydrogen, which can take place at lower temperatures, should therefore be taken into account for a study of switching from epoxidation to hydrogenation. Herein, an effort is mainly focused on clarifying the factors which define the reactions of epoxidation and hydrogenation of propene in the presence of H_2 and O_2 over Au/Ti-based oxide catalysts. Three types of support TiO_2, titanosilicates, and silicates without Ti and various preparation methods are employed for a comprehensive comparison.

2. Experimental

2.1. Preparation of support materials

As support materials, anatase TiO_2 microsphere (specific surface area: 54 $m^2 g^{-1}$), MCM-41 (a silicate with arrays of non-intersecting hexagonal channels, specific surface area: 1011 $m^2 g^{-1}$), Ti–TUD-1 (a 3-D mesoporous titanosilicate, specific surface area: 822 $m^2 g^{-1}$), and HPG (a hybrid porous organic/inorganic Ti–SiO_2 material with a structure as shown in Scheme 1, specific surface area: 627 $m^2 g^{-1}$) were chosen in the present study. Anatase TiO_2 microsphere was provided by the Institute of Process Engineering, Chinese Academy of Sciences, Beijing, China. It was calcined at 773 K for 4 h in air before the deposition of Au. HPG was provided by Toyota Central R & D Labs., Inc. and used as received. MCM-41 supported Au catalyst was prepared by one-pot synthesis, i.e. incorporating gold precursor compound in the process of MCM-41 synthesis.

The Ti–TUD-1 support with Ti/Si = 2/100 was prepared by a modified sol–gel method similar to that reported by Shan et al. [23]. In a typical synthesis, 29.8 g of triethanolamine (TEA, Wako, 98.0%) was added dropwise into a mixture of 0.678 g of tetrabutyl orthotitanate (TBOT, TCI, 99.0%) and 20.8 g of tetraethoxysilane (TEOS, Wako, 95.0%) with vigorous stirring for 2.0 h. The mixture was continuously stirred for another 1.0 h at room temperature; 19.8 g of H_2O was then added dropwise, and 14.7 g of tetraethylammonium hydroxide solution (TEAOH, Merck, 20%) was poured subsequently. After stirring for 24 h, the clear solution was transferred into a Teflon-lined autoclave and aged statically at 373 K for 40 h. The obtained solid was then finalized by calcination at 973 K for 10 h in air with a ramp rate of 1.0 K/min from room temperature to 973 K.

2.2. Preparation of Au catalysts

DP-NaOH method [24]: Typically, a solution of $HAuCl_4$ was prepared by dissolving the appropriate amount of $HAuCl_4{\cdot}4H_2O$ in 100 mL of deionized water. The solution was heated to 343 K, and the pH was adjusted to 7 by adding NaOH solution. The support was then added, and the suspension was stirred while the pH was maintained at 7.0 for 1.0 h. Then, the solid was separated by filtration with or without washing and dried under vacuum at room temperature for overnight or further calcined in air at given temperatures.

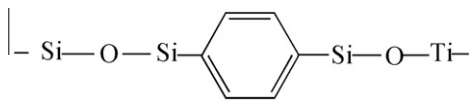

Scheme 1. The chemical structure of HPG support.

DP-NH_4OH method: An aqueous solution of $HAuCl_4{\cdot}4H_2O$ with 0.05 wt.% of nominal Au loading was added to Ti–TUD-1 support by incipient wetness impregnation. The sample was aged at room temperature for 2.0 h and then washed twice with an aqueous ammonia solution (15 mL, 1.0 M, pH of 11) and twice with deionized water (15 mL). The solid was centrifuged between each washing. The sample was dried under vacuum at room temperature for overnight and then calcined at given temperatures.

DP-urea method: A similar method reported by Zanella et al. [25] was applied to prepare Ti–TUD-1 supported Au catalysts with 0.05 wt.% of nominal Au loading by using urea ($CO(NH_2)_2$) as a precipitating agent; 0.5 g of Ti–TUD-1 support was added to 30 mL of an aqueous solution of $HAuCl_4$ (9.73×10^{-3} M) and 0.04 g of urea. The suspension thermo-stated at 353 K was vigorously stirred for 4.0 h in the absence of light. The cooled sample was then washed twice using 100 mL of deionized water with centrifuging between each washing. The sample was then dried under vacuum at room temperature for overnight and finally calcined at given temperatures.

SG method [26]: Solid grinding was used to deposit Au on HPG, TiO_2 microsphere, and Ti–TUD-1. The powder of the supports and the required amount of dimethyl Au(III) acetylacetonate [$(CH_3)_2$Au(acac)] were ground in an agate mortar in air for 20 min at room temperature, followed by reduction in 10 vol.% H_2/Ar stream or by calcination at 573 K.

2.3. Characterization of Au catalysts

The size of gold particles and its distribution for Au catalysts with higher Au loadings were observed with a JEOL JEM-2100 transmission electron microscopy operated at 200 kV. A small amount of powder sample was put into a test tube filled with 95% ethanol solution. After agitation under supersonic environment for a few minutes, one drop of the dispersion was dipped onto a carbon coated copper mesh and dried under light at room temperature. SEM-EDS was performed to estimate Au loadings of the catalysts with limited quantity.

Gold size and location information of a 0.05 wt.% Au/Ti–TUD-1 catalyst prepared by DP-NH_4OH method were obtained by high-angle annular dark field scanning transmission electron microscopy (HAADF–STEM) with a JEOL JEM-3000F transmission electron microscope equipped with a digitally processed STEM imaging system and electron energy-loss spectroscopy (EELS). Operating voltage was 300 kV, and resolution was about 0.20 nm. The catalyst sample was directly dispersed on a microgrid supported on a copper mesh without solvent.

2.4. Catalytic tests

Powder catalyst sample of 0.15 g was loaded into a vertical fixed-bed U-shaped quartz reactor. The feed gas was composed

Table 2
Reaction of propene with H_2 and O_2 mixture over supported Au catalysts (C_3H_6:O_2:H_2:Ar = 1:1:1:7, GHSV = 8000 h^{-1} mL $g_{cat.}^{-1}$).

Support	Catalyst number	Preparation method	Au loading (wt.%)	D_{Au} (nm)	Contaminants [a] (wt.%)	Calcination conditions	Temp. (K)	Conversion (%)		Selectivity (%)	
					Na or K			H_2	Py[b]	PO	C_3H_8
HPG	C.1-1	SG	≈0.31	1–13	No	RT[c], air	433	4	<1	25, 72 (CO_2)	
	C.1-2			–		423 K, H_2/Ar	373	13	5	No	100
	C.1-3			7.8		573 K, air	373	83	84	No	100
Ti–TUD-1	C.2-1	SG	≈0.31	–	No	RT, air	373	3.8	0.77	89, oxygenates	
	C.2-2			–		423 K, H_2/Ar	383	6.7	1.4	76	24
	C.2-3			4.3		573 K, air	373	16	1.3	76	24
	C.3-1	DP-NaOH	0.31[d]	3–15	Yes	Vacuum dry	453	22	4.5	41	53
	C.3-2			16		573 K, air	413	18	11	0	99
	C.3-3			21		873 K, air	453	38	21	Trace	99
	C.4	DP-NH_4OH	⩽0.04[e]	<2.0	No	573 K, air	433	73	35	–	99
	C.5	DP-urea	⩽0.05[e]	<2.0[f]	No	573 K, air	448	43	22	Trace	98
	C.6	DP-NaOH	⩽0.03[e]	<2.0[f]	No	Vacuum dry	443	38	30	4.7	92
[M]TiO_2[g]	C.7	SG	≈1.0	<2.0[f]	No	423 K, H_2/Ar	323–383	9–21	7–9	No	95–75
MCM-41	C.8	One-pot	<0.01	<2.0[f]	No	Vacuum dry	473	2.2	1.2	No	99

[a] Chloride contamination was negligible.
[b] Propene.
[c] Room temperature.
[d] Au loading was measured by SEM-EDS analysis.
[e] Au loadings were estimated by the previous samples.
[f] Au sizes were estimated.
[g] Anatase TiO_2 microsphere.

of propene, H_2, O_2, and Ar with a volume ratio of 10/10/10/70 and was passed through a catalyst bed under atmospheric pressure. All catalyst samples were not pretreated before catalytic tests. The hourly space velocity of the feed gas was 8000 h^{-1} mL $g_{cat.}^{-1}$. Reactants and products were analyzed by online GCs equipped with TCD (Porapak Q column) and FID (HR-20M column) detectors and with an auto-injector.

3. Results

Our previous works [7,11,12,15–17,27–29] and those of others [30–34] have clearly demonstrated that the presence of approximate 2.0–5.0 nm size Au nanoparticles in the proximity of isolated tetrahedral Ti sites is an important requirement for preparing an efficient propene epoxidation catalyst, regardless of the types of Ti-containing supports including anatase TiO_2 and titanosilicates with varying porosities from non-porous to high surface area mesoporous structure.

Propane formation at non-ignorable rates has often been observed in our recent experiments under the conditions of PO synthesis irrespective of supports and preparation methods used, as listed in Table 2. As a major product in the mixture of propene, H_2, and O_2, propane can be formed over Ti–TUD-1, HPG, MCM-41, and anatase TiO_2 microsphere in this work as well as over TiO_2 (P-25) [7,18] and SiO_2 [22] in the literatures, indicating that Ti, a prerequisite for PO synthesis, is not necessary for the hydrogenation of propene.

3.1. Propane formation over Au particles larger than 5.0 nm

Over Au catalysts in upper half of Table 2, propane formation greatly depends on calcination temperature of the catalyst precursors, which usually changes the size of Au particles and the content of residual chloride. Concerning Au on Ti–TUD-1 with an actual Au loading of 0.31 wt.% which produces both PO and propane, SG method (C.2) led to higher selectivity to PO than to propane while DP-NaOH method (C.3 in Table 2) led to higher propane selectivity, especially after high temperature calcination of the catalyst precursor in air. The SG catalyst calcined at 573 K (C.2-3 in Table 2) was composed of Au particles with a mean diameter of 4.3 nm and with 97% of Au particles smaller than 5.0 nm, indicating that three Au/Ti–TUD-1 catalysts prepared by SG method had the right size of Au particles for PO production.

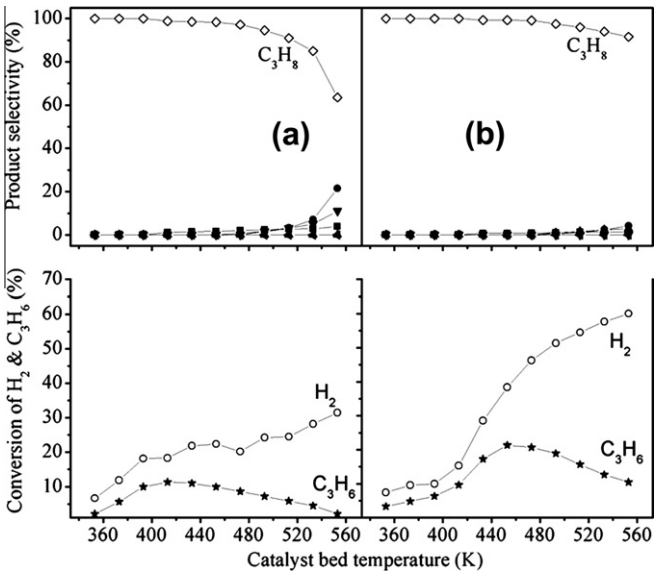

Fig. 1. Temperature dependence of the reaction of propene with H_2 and O_2 over 0.31 wt.% Au/Ti–TUD-1 prepared by DP-NaOH and by calcination in air at: (a) 573 K (C.3-2 in Table 2) and (b) 873 K (C.3–3 in Table 2). ■ PO, ● CO_2, ▲ acetone, ▼ propanal, ◇ C_3H_8, ◄ CH_3CHO, ○ H_2, ★ C_3H_6.

Since a considerable amount of PO was formed simultaneously with propane when the DP-NaOH catalyst was vacuum dried at room temperature (C.3-1 in Table 2) and possessed a wider size distribution of Au particles in the range of 3.0–15 nm, it can be assumed that PO production could be correlated with Au particles with diameters in the majority of 2.0–5.0 nm range. As depicted in Fig. 1, the Au catalyst became more active and selective for propane production when calcination temperature was elevated to 573 and then to 873 K and the mean diameter of Au particles

increased to 16 and 21 nm, respectively, implying that the larger the Au particles were, the more active and selective they were to propane. This is supported by the similar phenomena observed on a 0.31 wt.% Au/HPG catalyst prepared by SG method (C.1), as shown in the upper part of Table 2 and Fig. 2. It is noteworthy that the 0.31 wt.% Au/HPG catalyst calcined at 573 K in air (C.1-3 in Table 2) with a mean diameter of Au particles of 7.8 nm exposed Au nanoparticles outside of HPG channels as shown in Fig. 3 and presented a surprisingly high conversion of propene up to 84% with 100% selectivity to propane without the oxidation of H_2 to H_2O at temperatures $\leqslant$373 K.

In addition, air-dried SG Au/HPG catalyst (C.1-1 in Table 2) showed a wider size distribution of Au particles in the range from 1.0 to 13 nm. Seventy-seven percent of Au particles dropped to the 2.0–5.0 nm range and might account for 25% PO selectivity. A selectivity of 72% to CO_2 could be ascribed to a relatively high reaction temperature of 443 K.

The catalyst precursor was simply separated by filtration and not washed after deposition of Au for the above-mentioned 0.31 wt.% Au/Ti–TUD-1 DP-NaOH catalysts (C.2 in Table 2). The presence of chloride is known to cause remarkable aggregation of Au particles in the subsequent reduction treatment [35]. The larger Au particles for 0.31 wt.% Au/HPG calcined at 573 K (C.1-3 in Table 2) might be due to the hydrophobic property of the support when the SG method was employed to deposit Au via a weak interaction between –OH groups on the surfaces of HPG support and O atoms in Au complex $(CH_3)_2Au(O_2C_5H_7)$ [26]. High selectivity to propane over these catalysts agrees with the result reported by Chou et al. that Au particles of about 8.0 nm in diameter with 1.0 wt.% Au loading deposited onto P-25 TiO_2 favor the hydrogenation of propene in the presence of H_2 and O_2 [18].

In contrast to DP-NaOH method, the method of solid grinding does not bring contaminants (e.g. Na^+, K^+, Cl^-) in the catalyst and Au particles are deposited on both Si and Ti sites via the Au complex precursor [26]. High selectivity to propane over three DP-NaOH Au/Ti–TUD-1 catalysts (C.3) and three SG Au/HPG catalysts (C.1 in Table 2) indicates that propane formation over larger Au particles is not sensitive to the presence of alkalis and the location of Au particles.

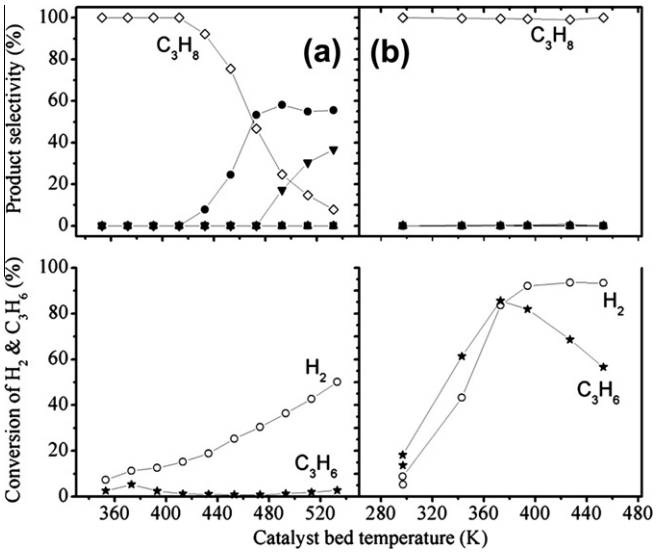

Fig. 2. Temperature dependence of the reaction of propene with H_2 and O_2 over 0.31 wt.% Au/HPG catalyst prepared by SG method and by: (a) reduction in 10 vol.% H_2/Ar at 423 K for 2.0 h (C.1-2 in Table 2) and (b) by calcination in air at 573 K for 3.0 h (C.1-3 in Table 2). ■ PO, ● CO_2, ▲ acetone, ▼propanal, ◇ C_3H_8, ◄ CH_3CHO, ○ H_2, ★ C_3H_6.

3.2. Propane formation on Au clusters smaller than 2.0 nm

As shown in the lower part of Table 2, high selectivity to propane with moderate conversions above 10% of propene was again obtained over the Au/Ti–TUD-1 catalysts with very low starting Au loadings in solution, such as 0.05 wt.% for DP-NH_4OH (C.4) and DP-urea (C.5), and 0.5 wt.% DP-NaOH (C.6 in Table 2) catalysts. Only very limited amount of alkalis could remain in these catalysts because NH_4OH solution and urea solution and extensive washing were applied to remove chloride in the process of catalyst preparation. Based on ICP analyses of co-precipitated Au catalysts, Na^+ and Cl^- impurities remained in DP Au catalysts were estimated to be below 100 ppm when extensive washing and calcination in air were performed [7]. HAADF–STEM observation of statistical 60 particles for the corresponding DP-NH_4OH catalyst confirmed that 75% of Au particles were smaller than 2.0 nm as shown in Fig. 4.

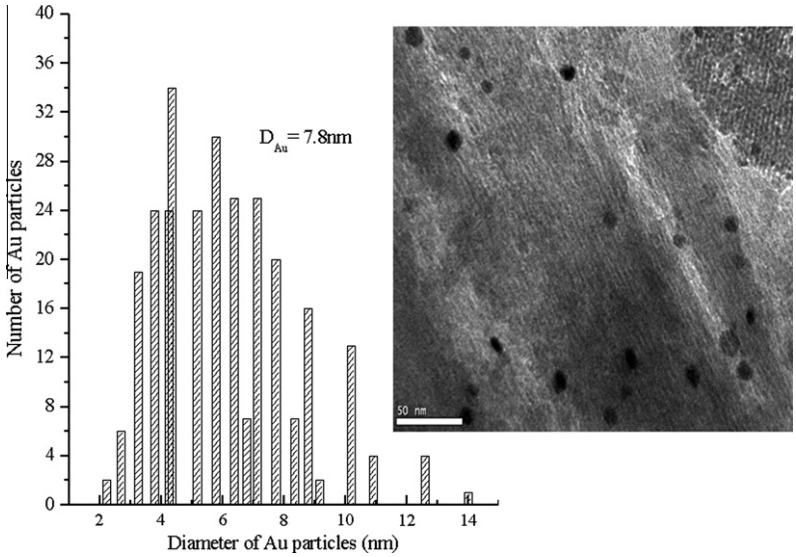

Fig. 3. HRTEM image and size distribution of Au particles for 0.31 wt.% Au/HPG catalyst prepared by SG method and by calcination in air at 573 K (C.1-3 in Table 2), D_{Au} denotes the mean diameter of Au particles.

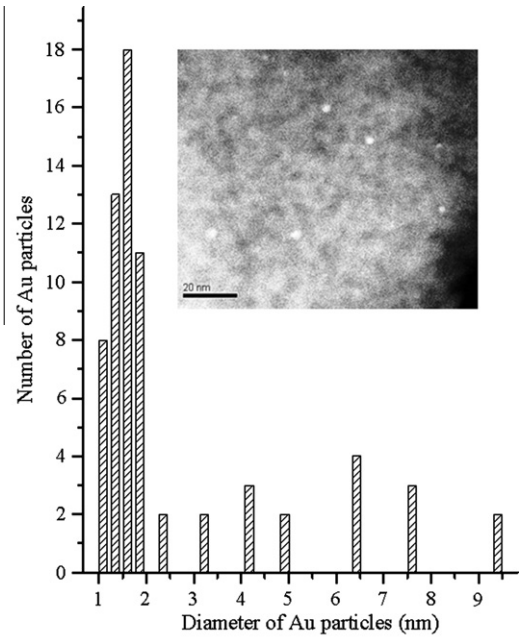

Fig. 4. HAADF–STEM image and the size distribution of Au particles for Au/Ti–TUD-1 prepared by DP-NH_4OH method and by calcination in air at 573 K (C.4 in Table 2). The Au loading in starting solution was 0.05 wt.%.

Results obtained by these three catalysts (C.4, C.5, C.6 in Table 2) support our earlier work on Au clusters (<2.0 nm) on P-25 TiO_2, which favors hydrogenation of propene in the absence of alkali ions (e.g. Na^+) [7]. The simultaneous formation of PO and propane was observed for the medium Au loadings and mean diameters of Au particles slightly smaller than 2.0 nm [7]). It can be suggested that Au particles larger than 2.0 nm mainly led to PO formation while those smaller than 2.0 nm to propane formation in the absence of alkalis.

EELS measurements of the oxide supports were carried out to obtain Ti composition mapping and to define the deposition sites of Au clusters on Ti–TUD-1 for the 0.05 wt.% Au/Ti–TUD-1 DP-NH_4OH catalyst (C.4 in Table 2). It was hard to find any correlation between tiny Au clusters and Ti sites, implying that these Au clusters were mostly located on the SiO_2 matrix but not concentrated in the proximity of Ti sites. This feature was different from that of Au catalysts with high metal loadings prepared by the DP method [17]. It is likely that very small amounts of gold entities are washed away from Ti sites. Au clusters on both Ti and Si sites can proceed the hydrogenation of propene.

So far, there is no report on the production of propane from propene in a mixture of H_2 and O_2 over Au/Ti-based oxides with a mean diameter of Au particles in 2.0–5.0 nm range. In principle, the reaction of propene hydrogenation can mainly take place on the Au/Ti-based oxides when Au particles are larger than 5.0 nm or smaller than 2.0 nm in the presence of H_2 and O_2.

3.3. Necessity of alkalis for PO formation over Au clusters smaller than 2.0 nm

In contrast to the switching of the product from PO to propane over Au/TiO_2 (P-25) with Au loadings below 0.10 wt.% and Au clusters smaller than 2.0 nm [7], high PO formation rate was observed for low loadings of Au (<0.02 wt.%) on a series of modified Ti–MCM-41 [17] and Au (<0.05 wt.%) on NH_4OH-treated microporous TS-1 [13,14] as well as Au (0.1 wt.%) on alkali-treated mesoporous TS-1 [10,20] and on Ba-promoted Ti–TUD support [19]. In the case of Au catalysts supported on micro and mesoporous TS-1 and Ti–TUD, the presence of Au clusters smaller than 2.0 nm was observed by HRTEM [10,13,14,19,20]. Gold located on tetrahedral TiO_4 sites is also indispensable for PO formation on Au clusters [19,20]. We noticed that there were some amount of alkali cations (Na^+ or K^+) remained in these catalysts [10,13,14,17,19,20], coming from the processing of supports and/or catalyst preparation. Table 3 lists the important epoxidation results, which were mostly obtained by our group and partly by other groups. It can be seen that PO can be principally produced on 2.0–5.0 nm Au particles no matter whether alkalis co-exist or not, while PO formation over Au clusters with mean diameters below 2.0 nm needs the assistance by alkali.

In order to investigate the role of alkali in reaction switching between hydrogenation and epoxidation of propene over gold clusters in a mixture of H_2 and O_2, anatase TiO_2 microsphere was chosen as the fourth support material to obtain Au clusters (<2.0 nm) with higher Au loadings. A given amount of anatase TiO_2 microsphere was firstly impregnated with NaOH solution to introduce 0.50 wt.% Na into the final catalyst. The SG method was applied to deposit 0.31 wt.% Au on Na-containing TiO_2, and the ground mixture was calcined at 573 K in air. As depicted in Fig. 5, 100% selectivity to PO was observed at 303 K over the corresponding catalyst. In fresh 0.31 wt.% Au/0.50 wt.% Na–TiO_2 microsphere catalyst, more than 76% of Au particles were smaller than 2.0 nm in diameter, suggesting that the key role of alkali (Na) is to shift hydrogenation to epoxidation over Au clusters. At 353 K, selectivity to PO decreased to 56% while selectivity to CO_2 increased considerably. When temperature was raised to 383 K, 82% selectivity to propane was obtained initially and propane selectivity was maintained up to 90% in 4.0 h on stream. TEM observation (Fig. 5b) showed a remarkable aggregation of Au particles over the catalyst after reaction. Twelve percentage of Au particles were smaller than 2.0 nm, 32% of gold particles were in the 2.0–5.0 nm range, and 56% of gold particles were larger than 5.0 nm, demonstrating the size dependence of Au particles in Au/Ti-based oxides on the reaction pathways of propene in a H_2 and O_2 mixture. The positive effect of surface alkalis (not only Na and K) on PO productivity and selectivity has already been demonstrated by a number of works [19,35–37] for Au catalysts composed mainly of Au particles with mean diameters of 2.0–5.0 nm.

3.4. Enhancement of propane formation by O_2

Over the catalyst of 1.0 wt.% Au deposited on anatase TiO_2 microsphere (C.7 in Table 2) by SG method, the reaction of propene with H_2 and O_2 was carried out after in situ reduction of the catalyst precursor in a flowing stream of 10 vol.% H_2 in Ar at 423 K for 2.0 h. As demonstrated in Fig. 6, propane was dominant in the temperature range of 298–383 K, except that trace PO was observed in the very beginning of the reaction. No product was found when H_2 was removed from the feed (propene + O_2) at 323 K, whereas propane was formed when O_2 was replaced with H_2 (propene + H_2) even at temperature down to 273 K. The mean size of Au particles was not measured but assumed to be below 2.0 nm through a comparison with the catalyst with Na in section 3.3.

More propane was formed when oxygen was added again. A continued increase in the conversion of propene with an increase in reaction temperature from 273 to 353 K indicates that the reaction of propene hydrogenation over Au catalyst is enhanced by O_2, in agreement with our result over an Au/MCM-41 with Au loading lower than 0.01 wt.% (C.8 in Table 2) and the result reported by Naito and Tanimoto over Au/SiO_2 catalysts with small Au loadings [22].

As depicted in Fig. 7, 0.31 wt.% Au/HPG calcined at 573 K (C.1–3 in Table 2) shows much higher propane formation rate in the feed

Table 3
Experimental results reported on the epoxidation of propene over Au catalysts (C_3H_6:O_2:H_2:Ar = 1:1:1:7).

Support	Au loading (wt.%)	D_{Au} (nm)	Contaminants [a]	Temp. (K)	Conversion (%)		Selectivity (%)		Formation rate (mol/g_{Au} h)	Refs.
			Na or K		H_2	Py	PO	C_3H_8	PO	
TiO_2 (P-25)	>0.4	2.2–2.4	No	323	3.2	1.1	99	No	0.002	[7][b]
	5.0	4.6	No	298–343	–	<0.6	>83	No	0.0008	[34][c]
	0.67	3.4	No	323	13.2	0.46	95	No	0.012	[27][d]
TS-1	0.84	3.8	Yes	373	7.9	0.71	>90	No	0.014	
TiO–SiO_2	0.60	3.2	Yes	423	32.1	4.5	>80	No	0.11	[28][d]
Mesopore TS-1	0.1	4.1	Yes	473	1.62	0.6	92	No	0.19	[20][e]
Ti–MCM-48	0.01	<2.0	No	–	–	–	Minor	Major	–	[16][d]
TS-2	0.04	2.1	Yes	373	5.8	0.68	>90	No	0.27	[27]
Ti–MCM-41	1.37	2.0	Yes	373	29.6	1.71	>90	No	0.02	
Ti–MCM-41	0.02	–	Yes	473	11	0.95	85	No	0.68	[17][d]
Ti–TUD	0.11	0.9	Yes	423	4.9	1.4	99	No	0.45	[19][f]
Micropore TS-1	0.05	<2	Yes	473	–	8.8	81	No	4.0	[13][f]
Mesopore TS-1	0.10	1.6	Yes	473	31.2	7.7	85	No	2.3	[20][e]

[a] Cl contamination was negligible.
[b] GHSV = 2000.
[c] 1800.
[d] 4000.
[e] 8000.
[f] 7000 h^{-1} mL $g_{cat.}^{-1}$.

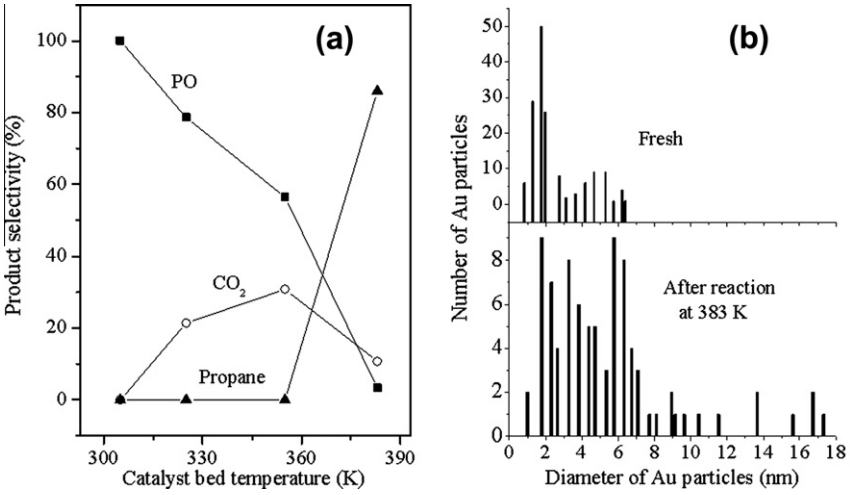

Fig. 5. (a) Product selectivity as a function of reaction temperature over 0.31 wt.% Au/0.50 wt.% Na–TiO_2 microsphere prepared by SG method and by calcination in air at 573 K. The data were obtained at each temperature after 1.0 h. (b) The size distribution of Au particles for the catalysts before and after reaction.

of propene: H_2:O_2:Ar = 1:1:1:7 than in the feed of H_2: propene: Ar = 1:1:8 without oxygen, showing that oxygen can also enhance the hydrogenation over larger Au nanoparticles by decreasing the activation energy from 33.6 to 16.2 kJ mol^{-1}. However, the rate markedly dropped when too much oxygen was co-fed.

4. Discussion

The most striking phenomenon related to Au catalysis is the strong dependence of the catalytic property on the size of Au particles and on the type of support materials. The switching of reaction between hydrogenation and epoxidation of propene again embodies this unique feature of Au catalysis. In the co-presence of H_2 and O_2, the occurrence of hydrogenation and epoxidation over Au/Ti-based oxides varies with the size of Au particles, revealing that Au particles of different sizes possess different capabilities in the chemical adsorption or dissociation of H_2 and O_2.

The experimental results reported previously and obtained in the present study clearly show that in the co-presence of H_2, O_2, and Au/Ti-based oxides as catalysts, the hydrogenation of propene producing propane mainly takes place over Au particles larger than 5 nm and over Au clusters smaller than 2.0 nm. In contrast, propane can scarcely formed over 2–5 nm Au particles, on which propene oxide is predominately produced. The hydrogenation over Au clusters requires the absence of alkalis or the concentration at least lower than 100 ppm [7]). The present work for the first time has proved that a certain amount of alkali can turn the hydrogenation of alkene to epoxidation reaction over Au clusters smaller than 2.0 nm.

4.1. Propene epoxidation and hydrogenation against hydrogen oxidation

Hydrogen oxidation to produce H_2O (combustion) is the fastest reaction among the reactions to occur in the gas feed containing C_3H_6, H_2, and O_2. Hydrogen is also consumed by both epoxidation and hydrogenation of propene with a stoichiometric ratio of 1:1. The occurrence of hydrogen combustion can be estimated by the ratio of H_2 conversion to propene conversion (see Tables 2 and 3). Hydrogen combustion takes place preferentially to the other

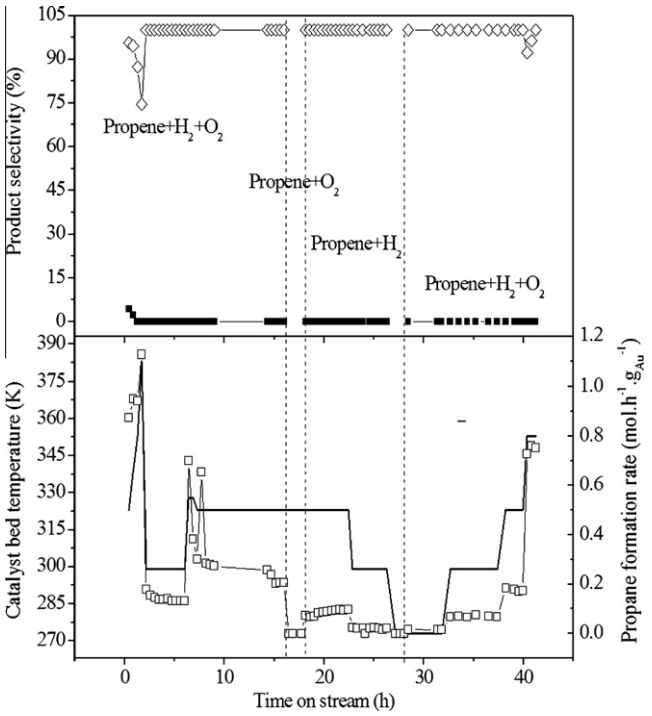

Fig. 6. Time on stream change of the reaction of propene and H_2 with or without O_2 over 1.0 wt.% Au/TiO_2 (anatase microsphere) catalyst prepared by SG method and by reduction in a flowing stream of 10 vol.% H_2 in Ar at 423 K for 2.0 h (C.7 in Table 2). ◇ propane selectivity; ■ PO selectivity; □ propane formation rate, – catalyst bed temperature.

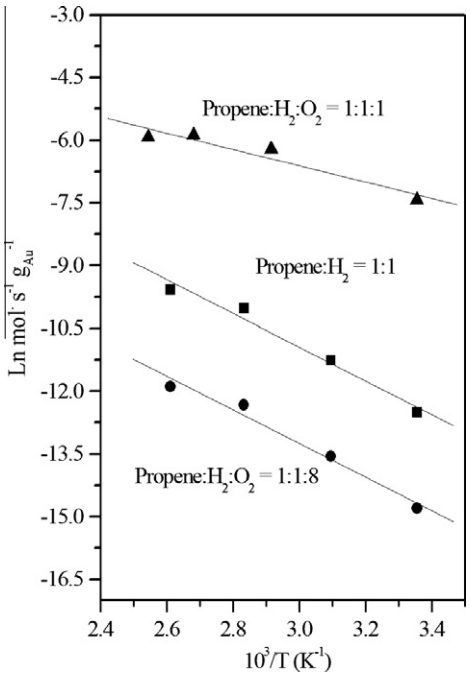

Fig. 7. Arrhenius plots of the reaction rates for propane formation over 0.31 wt.% Au/HPG catalyst prepared by SG method and by calcination at 573 K in air (C.1-3 in Table 2). Space velocity is 8000 mL $g_{cat.}^{-1}$ h^{-1}. The volume ratio of propene, H_2, O_2 and Ar is 1/1/1/7, 1/1/0/8 and 1/1/8/0, respectively.

reactions in all cases, with only one exception that occurs at temperatures ⩽373 K over a 0.31 wt.% Au/HPG catalyst prepared by the SG method and followed by calcination in air at 573 K (C.1-3 in Table 2). Although hydrogen combustion can be appreciably suppressed in the co-presence of propene [7], the rate of hydrogen combustion is still higher than the PO formation rate by a factor of 10 when PO is a dominant product. It is worth noting that the conversion ratio of H_2 to propene is limited to being below 3.0 in the case of propane formation no matter how much propene is converted. This implies that the epoxidation of propene and the combustion of H_2 are parallel reactions, whereas the hydrogenation of propene and the combustion of H_2 are competitive reactions.

Generally, for both epoxidation and hydrogenation of propene over Au catalysts, there is an optimum reaction temperature at which each catalyst presents the highest PO or propane yield (see Figs. 1 and 2). This optimal temperature is ⩽473 K as shown in the 8th column in Table 2 and the 5th column in Table 3, because H_2 combustion is more enhanced with an increase in temperature.

Up to now, we could some way identify the features that determine product selectivity in a complex system containing propene in a mixture of H_2 and O_2. A schematic representation for reaction switching is shown in Fig. 8 as functions of the mean diameters of Au particles, alkali content, and the reaction temperature.

4.2. Mutual enhancement by H_2 to epoxidation and by O_2 to hydrogenation

As a matter of fact, H_2 as a sacrificial reductant is needed to obtain high PO selectivity over Au particles smaller than 5.0 nm, although recent work has shown that a certain amount of PO can be obtained by Au nanoparticles or clusters with O_2 alone [10,38,39] with a help of H_2O (replacing H_2). On the other hand, the addition of oxygen to some extent can enhance the

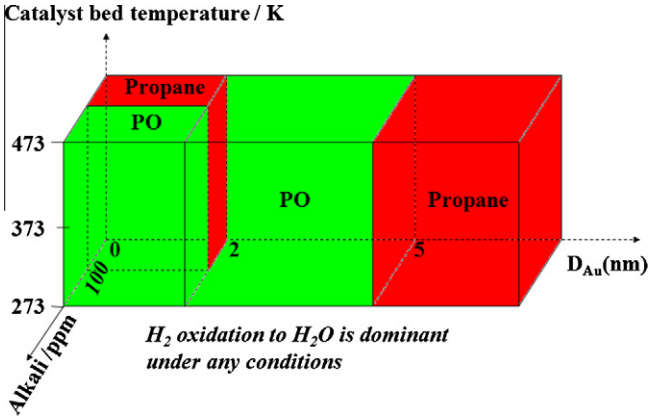

Fig. 8. The schematic representation for the hydrogenation and epoxidation of propene over Au/Ti-based oxides in the presence of H_2 and O_2.

hydrogenation reaction over both Au particles larger than 5.0 nm and clusters smaller than 2.0 nm.

H_2–D_2–$16O_2$–$18O_2$ and C_3H_6–H_2–$16O_2$–$18O_2$ reactions over Au/SiO_2 catalysts [22] suggest that oxygen molecules are not dissociatively chemisorbed but are transformed into peroxo-like adsorbed species, which enhance the dissociation of hydrogen molecule. The formation of the peroxo-like species is the most accepted hypothesis to explain the promotion of epoxidation by hydrogen or by H_2O over Au nanoparticles smaller 5.0 nm on Au/Ti catalysts [10,13,19,20,30,39,40–44]. Formation of Ti–OOH species during PO synthesis, one of the rate-determining steps in PO production estimated by kinetic studies [45–46], was confirmed by in situ UV–vis and EPR study [41]. One can assume that the hydroperoxy species are formed over Au catalysts during both the epoxidation and the hydrogenation of propene in a mixture of H_2 and O_2.

Table 4 presents the formation rates of PO and propane over the catalysts in Table 2 except for the catalysts of C.7 and C.8, because

Table 4
Formation rates of PO and propane over supported Au catalysts in Table 2 except for the catalysts of C.7 and C.8.

Catalyst number	Au loading (wt.%)	D_{Au} (nm)	Temp. (K)	Conversion of propene (%)	Selectivity (%)		Formation rate (mol/g_{Au} h)	
					PO	C_3H_8	PO	Propane
C.1-1	≈0.31	1–13	433	<1	25, 72 (CO_2)	0.29	–	
C.1-2		–	373	5	No	100	–	0.58
C.1-3		7.8	373	84	No	100	–	9.7
C.2-1	0.31	–	373	0.77	89	Oxygenates	0.079	–
C.2-3		4.3	373	1.3	76	24	0.11	0.036
C.3-1	0.31	3–15	453	4.5	41	53	0.21	0.27
C.3-2		16	413	11	0	99	–	1.3
C.3-3		21	453	21	Trace	99	–	2.4
C.4	⩽0.04	<2	433	35	–	99	–	31
C.5	⩽0.05	<2	448	22	Trace	98	–	15
C.6	⩽0.03	<2	443	30	4.7	92	1.7	33

there is high uncertainty in Au particle size for C.7 and the content of Au in C.8. The PO formation rates listed in Tables 3 and 4, in general, are greater over Au clusters than over Au nanoparticles if we neglect those data with high gold loadings. This agrees with our recent results on the better capability of Au clusters than that of Au nanoparticles for O_2 activation [10]. Interestingly, the PO formation rate (1.7 mol/g_{Au} h) over the catalyst of C.6 in Table 4 is comparable with the highest rates reported for alkali-promoted Au clusters (the last two columns in Table 3) [13,20], although the selectivity to PO is as low as 4.7%. This PO formation rate is still lower by a factor of 10 than the rate of propane formation over the same catalyst, implying that H_2 dissociation is much easier than O_2 activation on Au clusters in the co-presence of H_2 and O_2.

The work reported by Fujitani et al. has demonstrated that hydrogen dissociation may take place at the perimeter interfaces between Au clusters and TiO_2 [47]. The rate of HD formation by H_2 and D_2 exchange per unit weight of Au increased with a decrease in the size of Au particles and markedly increased below 2.0 nm. It can be assumed that the rapidly dissociated hydrogen on the perimeter interfaces of Au clusters and the support can readily react with propene adsorbed on the surfaces of Au and the support to form propane. Some part of dissociated hydrogen atoms may react with adsorbed O_2 at oxygen defect vacancies, on which H_2 dissociation is very slow [48], to form the hydroperoxy species that can in turn accelerate H_2 dissociation. The OOH species might be parallelly and competitively transferred at tetrahedrally coordinated Ti cation sites that can subsequently react with C_3H_6 adsorbed on the support to form PO in Au/Ti-based oxide system. One possibility for switching of hydrogenation to epoxidation over Au clusters by a certain amount of alkali is that more oxygen defect vacancies are created by the strong interaction between the added alkali and the Ti-containing support, as proposed by Panagiotopoulou and Kondarides [49] in the study on the effects of alkali addition to TiO_2 on the chemisorptive properties and water–gas shift (WGS) activity of supported noble metal catalysts (NM/X–TiO_2, NM = Ru, Pd, Pt, X = Li, Na, K, Cs).

Fujitani et al. have reported that the rate of H_2 dissociation per unit weight of Au is slowed down over 5.6 nm Au nanoparticles on TiO_2 by 30 times lower than that over 1.3 nm Au clusters [47]. Since propane is rarely reported as one of the products over the supported 2.0–5.0 nm Au nanoparticles in a mixture of propene with H_2 and O_2, one would speculate that the capability of 2.0–5.0 nm Au nanoparticles in H_2 dissociation is low and the formation of hydroperoxides might be the main driving force for H_2 dissociation. The limited isolated Ti^{4+} sites, compared with higher Au loadings, can only catch partial hydroperoxides to form Ti–OOH species which are indispensible for PO formation. The majority of hydroperoxides will directly decompose to H_2O, finally leading to the poor H_2 efficiency in many previously published works.

In addition, the rate of propane formation by Au/HPG catalyst with a mean diameter of Au particles of 7.8 nm (C.1-3) is higher than those by two TUD-1 supported Au catalysts even though the size of Au is in double. This can be ascribed to the hydrophobicity of the HPG material, on which the hydrogen combustion is markedly inhibited.

Hydrogen oxidation to water occurs at temperatures lower than CO oxidation on Au fine powder without a support [50], indicating that hydrogen can be dissociated on flat gold surfaces at temperatures below 473 K. The surfaces of Au particles larger than 5.0 nm may play a key role in H_2 dissociation in the co-presence of H_2 and O_2 over Au/Ti-based oxide catalysts. Part of propene molecules is adsorbed on the Au surfaces and readily react with dissociated H atoms to form propane. Over large Au particles, the number of perimeter Au–O–Ti sites that are selective to the epoxidation of propene markedly decreases.

4.3. Comparison with the epoxidation of higher alkenes in liquid phase

The epoxidation of alkenes higher than ethene with molecular oxygen alone remains a great challenge because of the hard competition against the allylic C–H activation. The epoxidation of propene [51], cyclohexene [52], cyclooctene [52,53], and stilbene [54] has been carried out using H_2O_2 or t-butyl hydroperoxide in liquid phase. Interestingly, 55 atoms of Au clusters were found to be a critical size in the epoxidation of styrene by using oxygen alone [55]. Liu et al. found that the epoxide yield over Au clusters with a mean diameter of 1.4 nm was higher than that over Au nanoparticles of 5.6 nm for the epoxidation of styrene using t-butyl hydroperoxide as the oxidant [56]. The catalytic performance of supported Au catalysts for the liquid phase epoxidation reactions shows some similarity to the results obtained in the present study for gas phase propene epoxidation. The liquid phase epoxidation rates reported so far mostly lie in the range of 0.1–1.5 mol/g_{Au} h [52–56], comparable with the rates of the gas phase propene epoxidation over 2.0–5.0 nm Au nanoparticles, 0.1–4.0 mol/g_{Au} h (Tables 3 and 4).

5. Conclusions

Over Au/Ti-based oxide catalysts in a mixture of propene, H_2, and O_2, three reactions mainly take place as follows: H_2 combustion, propene epoxidation, and propene hydrogenation. The hydrogen oxidation to form H_2O (combustion) can proceed under any conditions while switching of reactions between hydrogenation and epoxidation of propene occurs under specific circumstances. The hydrogenation of propene and H_2 combustion are competitive reactions, and the latter is remarkably depressed by the former,

whereas the epoxidation of propene and H_2 oxidation are parallel reactions. The ruling factors that determine the reaction pathways are investigated by employing different types of support materials and several catalyst preparation methods as well as by combining the experimental data available from the published work.

Over Au nanoparticles deposited in the proximity of tetrahedral Ti species, epoxidation of propene predominantly takes places with a size of 2.0–5.0 nm in a mixture of H_2 and O_2. The presence of alkalis promotes the epoxidation. The hydrogenation of propene usually prevails on Au nanoparticles larger than 5.0 nm no matter the presence of alkalis and on Au clusters smaller than 2.0 nm in the absence of alkalis irrespective of the location of Au clusters deposited either on Ti sites or on Si sites. A certain amount of alkalis can switch hydrogenation to epoxidation over Au clusters located on TiO_4 sites. The hydrogenation of propene is enhanced by the addition of oxygen, and the catalytic activity varies with the gas composition, the size of Au particles, and the type of supports.

Acknowledgments

Financial supports by Japan Science and Technology Agency to a CREST research project on gold catalysts and the Grow Programme from the World Gold Council (R.P. Project 0408) are greatly acknowledged. The authors also thank Dr. Shinji Inagaki and Dr. Yasutomo Goto of Toyota Central R & D Labs., Inc. Nagakute, Japan and Prof. Dan Wang of the Institute of Process Engineering, Chinese Academy of Sciences, Beijing, China, for providing us HPG and anatase TiO_2 microsphere, respectively.

References

[1] M. Haruta, N. Yamada, T. Kobayashi, S. Iijima, J. Catal. 115 (1989) 301.
[2] M. Haruta, S. Tsubota, T. Kobayashi, H. Kageyama, M.J. Genet, B. Delmon, J. Catal. 144 (1993) 175.
[3] G.J. Hutchings, M. Haruta, Appl. Catal. A: Gen. 291 (2005) 1.
[4] A. Stephen, K. Hashmi, G.J. Hutchings, Angew. Chem. Int. Ed. 45 (2006) 7896.
[5] G.C. Bond, C. Louis, D.T. Thompson, Catalysis by Gold, Imperial College Press, London, 2006. p. 161.
[6] G.J. Hutchings, W. Goodman, Top. Catal. 44 (2007) 1.
[7] T. Hayashi, K. Tanaka, M. Haruta, J. Catal. 178 (1998) 566.
[8] T.A. Nijhuis, M. Makkee, J.A. Moulijn, Bert M. Weckhuysen, Ind. Eng. Chem. Res. 45 (2006) 3447.
[9] C. Qi, Gold Bull. 41 (2008) 24.
[10] J. Huang, T. Akita, J. Faye, T. Fujitani, T. Takei, M. Haruta, Angew. Chem. Int. Ed. 48 (2009) 7862.
[11] A.K. Sinha, S. Seelan, S. Tsubota, M. Haruta, Angew. Chem. Int. Ed. 43 (2004) 1546.
[12] B. Chowdhury, J.J. Bravo-Suárez, M. Date, S. Tsubota, M. Haruta, Angew. Chem. Int. Ed. 45 (2006) 412.
[13] B. Taylor, J. Lauterbach, W.N. Delgass, Appl. Catal. A 291 (2005) 188.
[14] B. Taylor, J. Lauterbach, W.N. Delgass, Catal. Today 123 (2007) 50.
[15] A.K. Sinha, S. Seelan, S. Tsubota, M. Haruta, Top. Catal. 29 (2004) 95.
[16] B.S. Uphade, T. Akita, T. Nakamura, M. Haruta, J. Catal. 209 (2002) 331.
[17] C. Qi, T. Akita, M. Okumura, K. Kuraoka, M. Haruta, Appl. Catal. A 253 (2003) 75.
[18] J. Chou, N.R. Franklin, S-H. Baeck, T.F. Jaramillo, E.W. McFarland, Catal. Lett. 95 (2004) 107.
[19] J. Lu, X. Zhang, J.J. Bravo-Suárez, K.K. Bando, T. Fujitani, S.T. Oyama, J. Catal. 250 (2007) 350.
[20] J. Huang, T. Takei, T. Akita, H. Ohashi, M. Haruta, Appl. Catal. B 95 (2010) 430.
[21] S.C. Crisafulli, S. Minicò, G.G. Condorelli, A.D. Mauro, J. Mol. Catal. A 284 (2008) 24.
[22] S. Naito, M. Tanimoto, J. Chem. Soc. Chem. Commun. 12 (1988) 832.
[23] Z. Shan, J.C. Jansen, L. Marchese, Th. Maschmeyer, Microporous Mesoporous Mater. 48 (2001) 181.
[24] G.R. Bamwenda, S. Tsubota, T. Nakamura, M. Haruta, Catal. Lett. 44 (1997) 83.
[25] R. Zanella, L. Delannoy, C. Louis, Appl. Catal. A 291 (2005) 62.
[26] M. Ishida, N. Kinoshita, H. Okatsu, T. Akita, T. Takei, M. Haruta, Angew. Chem. Int. Ed. 47 (2008) 9265.
[27] B.S. Uphade, S. Tsubota, T. Hayashi, M. Haruta, Chem. Lett. (1998) 1277.
[28] M.P. Kapoor, A.K. Sinha, S. Seelan, S. Inagaki, S. Tsubota, H. Yoshida, M. Haruta, Chem. Commun. (2002) 2902.
[29] C. Qi, T. Akita, M. Okumura, M. Haruta, Appl. Catal. A 218 (2001) 81.
[30] T.A. Nijhuis, H. Huizinga, M. Makkee, J.A. Moulijn, Ind. Eng. Chem. Res. 38 (1999) 884.
[31] E.E. Stangland, K.B. Stavens, R.P. Andres, W.N. Delgass, J. Catal. 191 (2000) 332.
[32] G. Mul, A. Zwijnenburg, B. Linden, M. van der Makkee, J.A. Moulijn, J. Catal. 201 (2001) 128.
[33] N. Yap, R.P. Andres, W.N. Delgass, J. Catal. 226 (2004) 156.
[34] J. Chou, E.W. McFarland, Chem. Commun. (2004) 1648.
[35] B.S. Uphade, M. Okumura, S. Tsubota, M. Haruta, Appl. Catal. A 190 (2000) 43.
[36] L. Cumaranatunge, W.N. Delgass, J. Catal. 232 (2005) 38.
[37] E.E. Stangland, B. Taylor, R.P. Andres, W.N. Delgass, J. Phys. Chem. B 109 (2005) 232.
[38] S. Lee, L.M. Molina, M.L. Pez, J.A. Alonso, B. Hammer, B. Lee, S. Seifert, R.E. Winans, J.W. Elam, M.J. Pellin, S. Vajda, Angew. Chem. Int. Ed. 48 (2009) 1467.
[39] M. Ojeda, E. Iglesia, Chem. Commun. (2009) 352.
[40] A.K. Sinha, S. Seelan, M. Okumura, T. Akita, S. Tsubota, M. Haruta, J. Phys. Chem. B 109 (2005) 3956.
[41] B. Chowdhury, J.J. Bravo-Suárez, N. Mimura, J. Lu, K.K. Bando, S. Tsubota, M. Haruta, J. Phys. Chem. B 110 (2006) 22995.
[42] D.H. Wells, W.N. Delgass, K.T. Thomson, J. Catal. 225 (2004) 69.
[43] M. Okumura, Y. Kitagawa, K. Yamaguchi, T. Akita, S. Tsubota, M. Haruta, Chem. Lett. 32 (2003) 822.
[44] C. Sivandinarayana, T.V. Choudhardy, L.L. Daemen, J. Eckert, D.W. Goodman, J. Am. Chem. Soc. 126 (2004) 38.
[45] B. Taylor, J. Lauterbach, G.E. Blau, W.N. Delgass, J. Catal. 242 (2006) 142.
[46] J. Lu, X. Zhang, J.J. Bravo-Suárez, S. Tsubota, J. Gaudet, S.T. Oyama, Catal. Today 123 (2007) 189.
[47] T. Fujitani, N.T. Akita, M. Okumura, M. Haruta, Angew. Chem. Int. Ed. 48 (2009) 9515.
[48] Y. Yang, M. Sushchikh, G. Mills, H. Metiu, E. McFarland, Appl. Surf. Sci. 229 (2004) 346.
[49] P. Panagiotopoulou, D.I. Kondarides, J. Catal. 267 (2009) 57.
[50] M. Haruta, T. Kobayashi, H. Sano, N. Yamada, Chem. Lett. (1987) 405.
[51] E. Klemm, E. Dietzsch, T. Schwarz, T. Kruppa, A. Lange, de. Oliveira, F. Becker, G. Markowz, S. Schirrmeister, R. Schütte, K.J. Caspary, F. Schüth, D. Hönicke, Ind. Eng. Chem. Res. 47 (2008) 2086.
[52] M.D. Hughes, Y.-J. Xu, P. Jenkins, P. McMorn, P. Landon, D.I. Enache, A.F. Carley, G.A. Attard, G.J. Hutchings, F. King, E.H. Stitt, P. Johnston, K. Griffin, C.J. Kiely, Nature 437 (2005) 1132.
[53] S. Bawaked, N.F. Dummer, N. Dimitratos, D. Bethell, Q. He, C.J. Kiely, G.J. Hutchings, Green Chem. 11 (2009) 1037.
[54] V. Mendez, K. Guillois, S. Daniele, A. Tuel, V. Caps, Dalton Trans. 39 (2010) 8457.
[55] M. Turner, V.B. Golovko, O.P.H. Vaughan, P. Abdulkin, A. Berenguer-Murcia, M.S. Tikhov, B.F.G. Johnson, R.M. Lambert, Nature 454 (2008) 981.
[56] Y. Liu, H. Tsunoyama, T. Akita, T. Tsukuda, Chem. Comun. 46 (2010) 550.